γD-Crystallin–Associated Protein Aggregation and Lens Fiber Cell Denucleation

Kaijun Wang,[1,2,3] *Catherine Cheng,*[3,4] *Lin Li,*[1] *Haiquan Liu,*[1] *Qingling Huang,*[5] *Chun-hong Xia,*[1] *Ke Yao,*[2] *Peiqing Sun,*[6] *Joseph Horwitz,*[5] *and Xiaohua Gong*[1,4]

PURPOSE. To understand the underlying molecular mechanism for a dominant cataract caused by a point mutation in the γD-crystallin gene.

METHODS. A dominant cataractous mouse line was identified from chemically induced mouse mutations by phenotypic screening with slit lamp examination. Genomewide linkage analysis and DNA sequencing were used to determine the causative gene mutation. Histology, immunohistochemistry, Western blotting, and in vitro transfection studies were used to characterize mutant lenses.

RESULTS. Cataracts in mutant mice were caused by a point mutation in the γD-crystallin gene (γD-V76D). Intranuclear γ-crystallin aggregates, incomplete denucleation, and decreased connexins were observed in mutant lens fiber cells. Mutant γD-V76D proteins became less soluble in the lens, and structural modeling suggested that the substituted aspartic acid residue (D) altered hydrogen bond formation and surface electrostatic potential of the protein. Unexpectedly, the formation of cold cataracts, which occurred in wild-type lenses at low temperature, was abolished in γD-V76D mutant lenses. In vitro transfection studies revealed that wild-type γD proteins were uniformly distributed in the cytosol and nucleus of transfected cells, whereas γD-V76D proteins formed cytosolic and nuclear aggregates.

CONCLUSIONS. Mutant γD-V76D reduces protein solubility in the lens and forms substantial intranuclear aggregates that disrupt the denucleation process of inner lens fiber cells. Sustained fiber cell nuclei and nuclear remnants scatter light, whereas other downstream events, such as decreased connexins, presumably disrupt gap junction communication and lens homeostasis, further contributing to the cataract phenotype in mutant lenses. This work also suggests that γD-crystallin is one of the crucial components for the formation of cold cataracts in vivo. (*Invest Ophthalmol Vis Sci.* 2007;48:3719–3728) DOI:10.1167/iovs.06-1487

The eye lens contains a high concentration of crystallin proteins (α, β, and γ classes). It is commonly thought that crystallin proteins display repulsive interactions that not only prevent the risk of protein crystallization or aggregation but also contribute to even, dense packing in the cytosol required for lens transparency and a high refractive index.[1] The lens grows continuously throughout life. At the cellular level, the lens is composed of a bulk of elongated fiber cells covered by a monolayer of epithelial cells on the anterior surface. Surface epithelial cells differentiate into elongated fiber cells at the lens equator, and newly differentiated fiber cells surround previous generations of fiber cells in a concentric manner.[2] Organelle degradation during lens fiber cell maturation is essential for minimizing light scattering to maintain lens transparency. Lens inner fiber cells eliminate all intracellular organelles, including nuclei, endoplasmic reticulum, Golgi apparatus, and mitochondria.[3] Therefore, inner mature fibers depend on lens peripheral fiber cells and epithelial cells to supply metabolites, ions, and water through intercellular gap junction channels.[4,5]

Cataracts, named for any opacity in the lens, are the leading cause of vision impairment in the world. Studies of hereditary cataracts caused by mutated genes have led to some mechanistic understanding of cataract formation.[6] Defects in fiber cell maturation, such as incomplete denucleation, are associated with cataracts caused by mutations of connexins, crystallins, and DNAse II-like acid DNAse (*DLAD*) genes.[7–9] It remains unclear whether apoptotic machinery is involved in fiber cell maturation.[10–12] However, lens fiber cells never undergo apoptosis; rather, they become mature fibers by losing intracellular organelles. The molecular mechanisms for initiating and executing organelle degradation in lens fiber cells remain largely unknown.[13]

α-Crystallins (αA and αB subunits) are molecular chaperones that belong to the small heat shock protein family.[14] It has been suggested that α-crystallins prevent abnormal protein aggregation by directly binding to "denatured" proteins to ensure lifelong lens transparency.[15] Both β- and γ-crystallins are lens structural proteins, and they belong to a related β/γ superfamily that shares a common structural motif: a Greek-key domain.[16] Six members of the β-crystallin family are divided into two groups: three acidic isoforms (βA1–βA3) and three basic isoforms (βB1–βB3). The γ-crystallin family has seven members, γA to γF and γS. The γA to γF proteins are encoded by a cluster of genes on mouse chromosome 1 or human chromosome 2, whereas γS is located on mouse chromosome 16 or human chromosome 7. Recently, γN-crystallin, a β/γ-hybrid protein, was identified.[17] It is unclear whether β/γ-crystallins perform functions in addition to acting as necessary structural components for the lens.

Here we report studies of a dominant cataractous mouse line (*L23*) identified from ethylnitrosourea (ENU)-induced germline mutations in the C57BL/6J strain background. A missense mutation of the *CrygD* (γD-crystallin) gene, which results in the substitution of valine (V) at codon 76 by an aspartic

Corresponding author: Xiaohua Gong, Vision Science Program and School of Optometry, University of California, 693 Minor Hall, Berkeley, CA 94720-2020; xgong@berkeley.edu.

acid (D; γD-V76D), leads to whole lens cataracts in heterozygous mutant mice and posterior ruptured lenses in homozygous mutant mice. This work provides some mechanistic evidence to explain why and how γD-V76D mutant proteins cause distinct lens phenotypes and direct evidence for the involvement of γD-crystallin in the formation of lens cold cataracts, defined as lens opacities induced by low temperature, in vivo.

MATERIALS AND METHODS

Phenotypic Screening, Genomic Linkage Analysis, and Causative Gene Identification

Mouse care and breeding were performed in accordance with the animal care and use committee–approved animal protocol (University of California at Berkeley) and the ARVO Statement for the Use of Animals in Ophthalmic and Vision Research. ENU-mutagenized mice were produced as described previously.[18] Mouse pupils were dilated by 1% atropine and 1% phenylephrine before mice were examined by slit lamp for lens clarity. Mouse breeding, genomic linkage analysis, and DNA sequencing were performed according to previously described approaches.[19]

Histology and Immunohistochemical Staining

Enucleated eyeballs opened at the anterior chamber or posterior vitreous were immersed in a fixative solution containing 2% glutaraldehyde and 2.5% formaldehyde in 0.1 M cacodylate buffer (pH 7.2) at room temperature for 5 days. Samples were postfixed in 1% aqueous OsO_4, stained en bloc with 2% aqueous uranyl acetate, and dehydrated through graded acetone. Samples were embedded in epoxy resin (eponate 12-araldite 502; Ted Pella, Redding, CA). Lens sections (1 μm) across the equatorial plane were collected on glass slides and stained with toluidine-blue. Bright-field images were acquired through a light microscope (Axiovert 200; Carl Zeiss, Oberkochen, Germany) with a digital camera. A previously described procedure was used for preparing lens cryosections for immunohistochemical staining.[20] A laser confocal microscope (Leica; Wetzlar, Germany) was used to collect fluorescent images.

Cold Cataracts and Quantification of Aggregates and Lens Proteins

Fresh lenses, dissected from enucleated eyeballs, were immediately immersed in PBS at 4°C. For histologic samples, lenses were immersed into a fixative solution containing 2% glutaraldehyde and 2.5% formaldehyde in 0.1 M cacodylate buffer (pH 7.2) at 4°C to induce cold cataracts or at 37°C to prevent cold cataracts for 3 days. A standard method was used for preparing toluidine blue–stained sections.

Quantification of Aggregates Induced by Low Temperature. Nine squares (50 μm × 50 μm) from an area 200 to 300 μm away from the lens capsules of wild-type, γD (V76D/+), and γD (V76D/V76D) lens histology sections were chosen for cold cataract analysis. Cold-induced aggregates were counted using Scion Image for Windows. Using the threshold function of the software, the contrast was adjusted for each square so that the aggregates are clearly visible and separate from neighboring aggregates. Then using the analyze particles function (minimum particle size, 5; maximum particle size, 300), cold cataract aggregates in each square were quantified and recorded. The average number of aggregates per square per genotype and the SE were plotted in Excel for comparison.

Quantification of Lens Proteins. For measuring lens total, water-soluble, and water-insoluble proteins, lenses were collected from three wild-type and three homozygous mutant mice at postnatal day (P) 5. Lens total proteins were prepared by homogenizing a pair of lenses from one mouse in 150 μL of 0.1 M NaCl with 50 mM sodium phosphate buffer (pH 7.2) per 1 mg wet lens weight, followed by centrifugation at 15,000 rpm for 15 minutes at 4°C. The supernatant was collected as lens water-soluble proteins, and the pellet was lens water-insoluble proteins. All protein samples were resuspended in phosphate buffer with 2% SDS, and protein concentration was measured by protein assay (DC Protein Assay Kit; Bio-Rad, Hercules, CA). A BSA standard curve was used to calculate the amount of total, water-soluble, and water-insoluble proteins. Final results were the average of three samples from three wild-type and three mutant mice. The percentage of water-soluble or water-insoluble proteins in the total proteins and the SE were calculated and graphed in Excel.

Cloning and Expression Plasmid Construction

Lens total RNA was isolated from wild-type and homozygous mutant lenses with reagent (TRIzol; Invitrogen, Carlsbad, CA). Two micrograms of total RNA was used to generate cDNA (Superscript First-Strand Synthesis System for RT-PCR Kit; Invitrogen, Carlsbad, CA). cDNAs that cover the entire coding regions of γD- and γB-crystallins were amplified by pfx DNA polymerase (Platinum; Invitrogen). A pair of primers (γD, *Eco*RI-CGGAATTCCCATGGGGAAGA [sense]; γD, *Bam*H1-CGGGATCCCCACCTCCACCGTAGAAATCC [antisense]) was used to amplify wild-type γD and mutant γD-V76D cDNAs. Other primers (γB, *Eco*RI-CGGAATTCAGATGGGAAAG [sense]; γB, *Bam*H1-
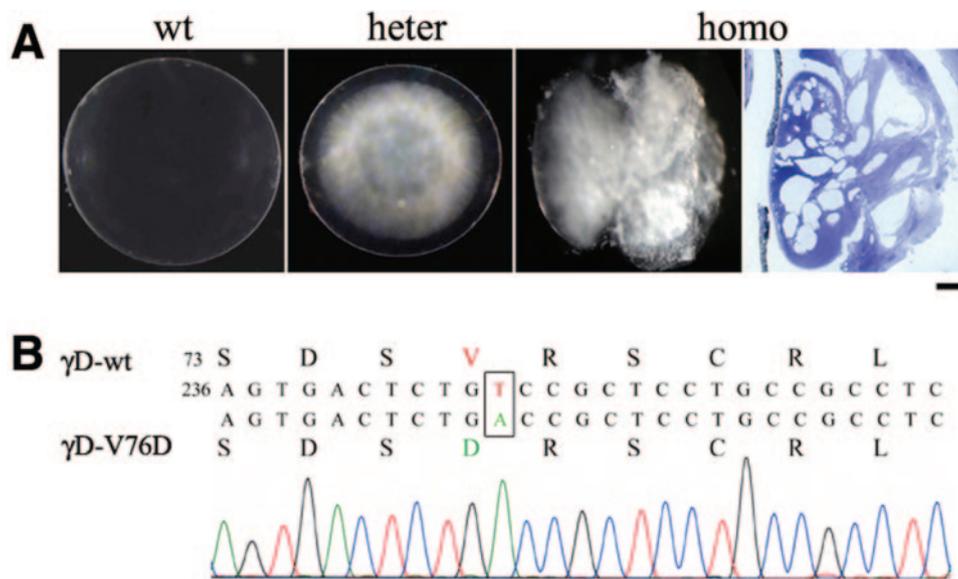

FIGURE 1.   γD-V76D point mutation leads to dominant cataracts in the *L23* mice. (**A**) Fresh lenses from 3-week-old mice. The heterozygous mutant lens (heter) developed a whole cataract and was slightly smaller than the wild-type (wt) lens. The homozygous mutant lens (homo) had a ruptured posterior, and a lens histologic section displayed "vacuoles" and disrupted fiber cells (*right*). Scale bar, 300 μm. (**B**) DNA sequencing data confirmed a T to A missense mutation in the *CrygD* gene, resulting in Val76 being substituted by an aspartic acid (γD-V76D).

CGGGATCCCCACCTCCACCGTAAAAATC [antisense]) were used for the amplification of wild-type γB and mutant γB-I4F cDNAs. γD and γB cDNAs were subcloned into the *Eco*RI and *Bam*H1 sites of the PDsRed1-N1 vector, with the 3′-ends of cDNAs in-frame with the red fluorescent protein (*RFP*) gene.

Immortalized Lens Epithelial Cells and Cell Transfection

Generation of Immortalized Lens Epithelial Cells. Mouse lenses were dissected from 10-day-old mice and trypsinized for 30 minutes at 37°C to dissociate any cells that were attached to the outer surface of the lens capsule. These lenses were washed with PBS three times and were examined under a microscope to confirm that they were intact without other attached cells. Thereafter, the lens capsule was mechanically broken with a tip and was trypsinized again for 10 minutes at 37°C to dissociate the lens cells. Suspended epithelial cells were plated on culture dishes for a few days before infection with a recombinant retrovirus,[21] BabeHygro-E6E7PGK-H-RasV12, which expresses the oncogenes *E6E7* and *H-RasV12*.[22,23] Hygromycin-resistant cells are immortalized lens epithelial cells that retain high-proliferation properties for more than 20 passages.

Cell Transfection. Immortalized lens epithelial cells were plated onto 35-mm dishes 24 hours before transfection. Cells were between 60% and 70% confluent in the 35-mm dish on the day of transfection. Plasmid DNA (2 μg each plasmid per 35-mm dish) was

transfected into these cells according to a procedure provided by the manufacturer (Superfect; Qiagen, Valencia, CA). Cells were incubated with transfection mixtures for 3 hours under normal growth condition, and fresh culture medium was added after 3 hours. Transfected cells were observed for RFP signals after 48 hours and then were mounted with mounting medium for fluorescence with DAPI (Vector Laboratories, Inc., Burlingame, CA). Images were collected by a fluorescence microscope (Axiovert 200; Zeiss).

Western Blot Analysis of Lens Proteins

Water-soluble and water-insoluble proteins were prepared. Two lenses were homogenized in 0.1 M NaCl with 50 mM sodium phosphate buffer (pH 7) at a ratio of 40 mg/mL (lens wet weight/solution volume) and were centrifuged at 15,000 rpm for 15 minutes at 4°C to separate water-soluble proteins in the supernatant from water-insoluble proteins in the pellet. The pellet was washed with the same buffer twice and was dissolved in 50 μL sample buffer (60 mM Tris, pH 6.8, 2% SDS, 10% glycerol, 5% β-mercaptoethanol, and 0.001% bromophenol blue). Total lens proteins were prepared as follows. Enucleated fresh lenses were weighed and homogenized directly in the sample buffer (60 mM Tris, pH 6.8, 2% SDS, 10% glycerol, 5% β-mercaptoethanol, and 0.001% bromophenol blue) at a ratio of 40 mg/mL (lens wet weight/solution volume). Equal volumes (20 μL) of samples were loaded on a 12.5% SDS-PAGE gel for separation, and separated proteins were transferred to a polyvinylidene (PVDF) membrane (Bio-Rad), which was detected

FIGURE 2. γD-V76D mutation inhibits fiber cell denucleation. (**A**) Histologic analysis of wild-type γD (+/+), heterozygous γD (V76D/+), and homozygous γD (V76D/V76D) lenses. At P1, heterozygous and homozygous lens sections were similar to wild-type lens sections. At P7, however, the posterior region of the homozygous lens showed sustained cell nuclei (*arrows*) and vacuole-like (*arrowhead*) defects that were not present in posterior regions of wild-type or heterozygous lenses. (**B**) DAPI-stained lens frozen sections showed that cellular nuclei were predominantly eliminated in center mature fiber cells of wild-type γD (+/+) lenses at P1 and P21. However, either intact nuclei or nuclear remnants were present in those of γD (V76D/+) lenses, and many more intact nuclei were present in the P1 γD (V76D/V76D) lens. (**C**) Ethidium bromide–stained DNA gel showed that genomic DNA was present in the lens nuclear regions (approximately 60% of total lens in weight) of P21 γD (V76D/+) lenses, but not in those of wild-type (+/+) lenses. Two lenses from each genotype were used for genomic DNA isolation, and all isolated DNA was loaded on the agarose gel. A 1-kb DNA ladder marker was used. Scale bars: (**A**) 100 μm (P1) and 20 μm (P7); (**B**) 100 μm.
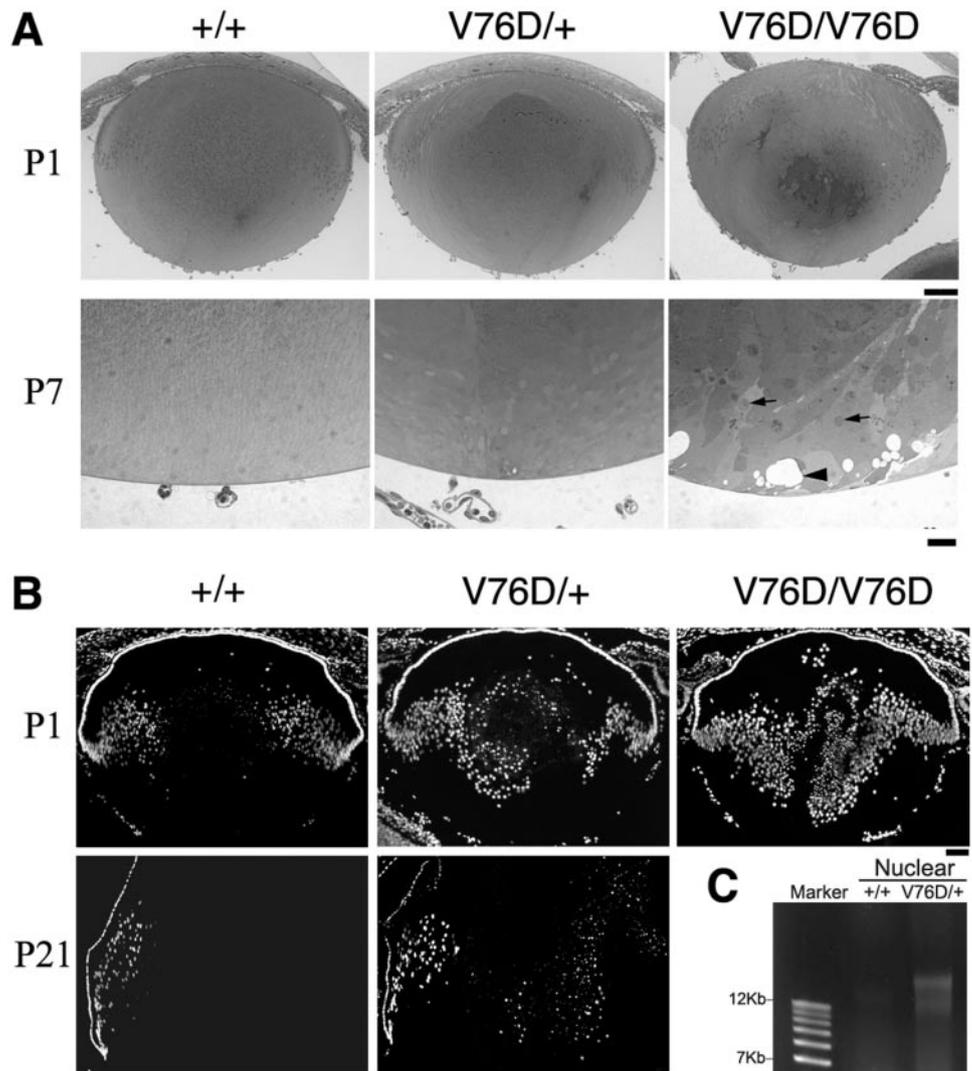
by Western blotting with rabbit polyclonal antibodies for actin, MP26, α3, and α8 connexins.

RESULTS

Cataracts and Ruptured Lenses in Mutant Mice

The *L23* mutant line was identified from ENU-induced G1 mutant mice. Heterozygous mice developed whole cataracts with slightly small lenses, whereas homozygous mice had severely deformed lenses that underwent posterior rupture (Fig. 1A). With the use of 42 meioses from a backcross between heterozygous B6-*L23*/+ and wild-type C3H/HeJ mice, we mapped the *L23* mutation to chromosome 1 near the linkage marker D1Mit380, close to the crystallin *Cryg* gene cluster, which includes γA, γB, γC, γD, γE, and γF genes. DNA-sequencing analysis was performed to verify the coding regions of these six γ-crystallin genes. A missense mutation (T to A) was found in the *CrygD* gene, which resulted in the replacement of valine at codon 76 by an aspartic acid (γD-V76D; Fig. 1B). No mutations were detected in the other five γ-crystallin isoforms (data not shown). The *L23* heterozygous and homozygous mice are hereafter referred to as γD (V76D/+) and γD (V76D/V76D), respectively.

Incomplete Denucleation in Mutant Lens Fiber Cells

Histology data revealed intact homozygous γD (V76D/V76D) lenses at P1, similar to heterozygous γD (V76D/+) and wild-type lenses (Fig. 2A). However, by P7, the posterior region of homozygous lenses displayed obvious abnormalities, such as vacuoles and cells with nuclei, compared with wild-type or heterozygous lenses (Fig. 2A). Thus, homozygous lenses probably undergo posterior rupture after P7. DAPI-stained lens frozen sections confirmed that inner fiber cells of P1 wild-type lenses underwent the maturation process to eliminate cell nuclei (Fig. 2B). However, many inner fiber cells of P1 γD (V76D/+) lenses had nuclear remnants or intact nuclei, and most inner fiber cells of P1 γD (V76D/V76D) lenses contained intact nuclei. At P21, compared with wild-type lenses, inner fiber cells of γD (V76D/+) lenses still had nuclear remnants (Fig. 2B). Moreover, genomic DNA was isolated from the nu-

clear region (approximately 60% of total lens in weight) of P21 γD (V76D/+) lenses, whereas the nuclear regions of wild-type lenses had no detectable genomic DNA (Fig. 2C). We were unable to evaluate inner mature fiber cells of P21 homozygous lenses because of posterior rupture (Fig. 1A). These data suggest that the γD-V76D mutation inhibits the denucleation of lens fiber cells.

Intranuclear γ-Crystallin Aggregates Caused by the γD-V76D Mutation

Toluidine-blue–stained histologic sections revealed the typical morphology of fiber cell nuclei of wild-type lenses (Fig. 3A). However, darkly stained aggregates appeared in fiber cell nuclei of γD (V76D/V76D) lenses (Fig. 3B). Immunostaining of frozen lens sections with an anti–γ-crystallin antibody revealed γ-crystallin protein aggregates in the fiber cell nuclei of γD (V76D/V76D) lenses (Fig. 3D) but not in those of wild-type lenses (Fig. 3C).

Cytosolic protein aggregates of wild-type lenses are known to be associated with cold cataracts. When histology sections were prepared from lenses that were fixed at room temperature rather than at 37°C, many small aggregates (black spots) were observed in the cytosol of inner fiber cells of wild-type lens sections (Fig. 3A), but not in those of γD (V76D/V76D) lens sections (Fig. 3B). This result suggests that mutant γD-V76D proteins affect protein aggregation or cold cataracts induced by low temperature. Therefore, we examined low temperature–induced lens protein aggregates and cataracts in these lenses.

Mutation Abolished Cold Cataract and Reduced Water-Soluble Proteins and Connexins

A previous study reported that the aggregation of crystallin proteins was associated with cold cataracts in young rat lenses.[24] To examine cold cataracts in mouse lenses, we processed enucleated mouse lenses at 4°C. Unlike wild-type lenses that formed cold-induced protein aggregates in inner fiber cells, heterozygous mutant lenses displayed a reduced level of cold-induced protein aggregates, and homozygous mutant lenses showed almost no cold-induced protein aggregates (Fig. 4A). When lenses were processed at 37°C, protein aggregates
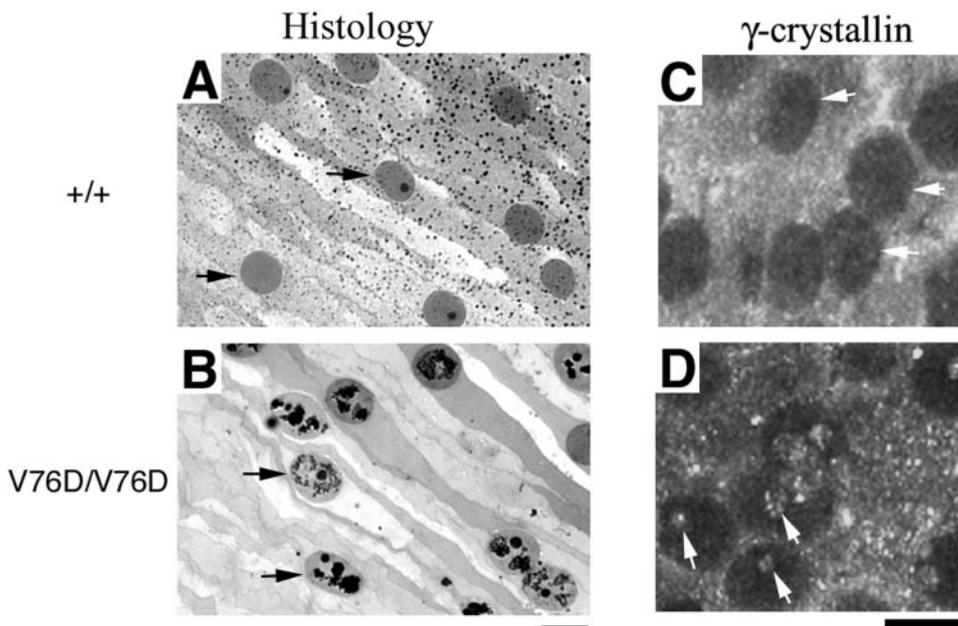

FIGURE 3. Aggregates in fiber cell nuclei are recognized by anti–γ-crystallin antibodies. (**A**) A P7 wild-type γD (+/+) lens section showed normal nuclei (*arrows*) in differentiated fiber cells with cytosolic aggregates (*darkly stained dots*). (**B**) P7 γD (V76D/V76D) lens section showed large aggregates (*arrows*) in nuclei of differentiated fiber cells without cytosolic aggregates. (**C**) Immunostaining confirmed the absence of γ-crystallin protein aggregates in fiber cell nuclei (*white arrows*) of P1 wild-type lenses. (**D**) Immunostaining revealed γ-crystallin protein aggregates in fiber cell nuclei (*white arrows*) of P1 γD (V76D/V76D) lenses. Scale bars, 10 μm.

FIGURE 4. Absence of cold-induced aggregates and cold cataracts in mutant γD-V76D lenses. (**A**) Toluidine blue–stained section showed that the P1 wild-type γD (+/+) lens formed typical aggregates (*darkly stained dots*) induced by low temperature (4°C) in inner fiber cells. However, the P1 heterozygous γD (V76D/+) lens had fewer cold-induced aggregates, and the P1 homozygous γD (V76D/V76D) lens had almost no aggregates in lens fiber cells. *Insets* are enlarged views of the areas indicated by *white arrows*. These aggregates were not observed in lens sections prepared from a fixation at 37°C. Scale bar, 50 μm. (**B**) Cold-induced aggregates were quantified based on the average number of aggregates among nine randomly selected squares (50 μm × 50 μm) of similar regions (approximately 200–300 μm from lens capsule) from histologic sections of wild-type (wt), γD (V76D/+), and γD (V76D/V76D) lenses. (**C**) Fresh lenses of P3 wild-type, γD (+/+), and γD (V76D/V76D) mice. Images were taken 5 minutes after these lenses were immersed in PBS buffer maintained at 4°C or 37°C. (**D**) Comparison of water-soluble and water-insoluble protein amount in P5 wild-type (wt) and homozygous mutant γD (V76D/V76D) lenses. Percentages of water-soluble and water-insoluble proteins in lens total proteins were graphed. The loss of soluble proteins in mutant lenses was accompanied by an increase of water-insoluble proteins.
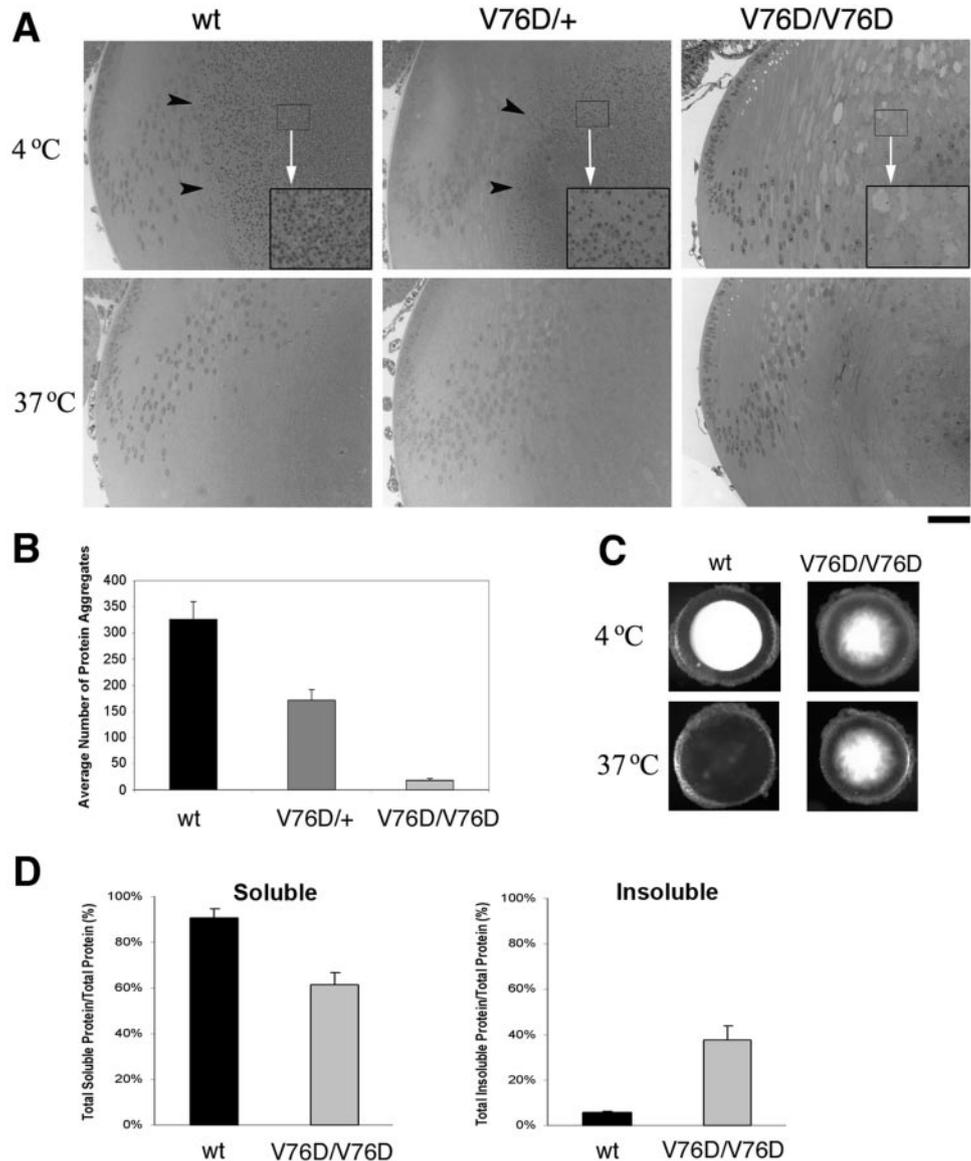
were not observed in any of these lenses. We directly quantified the number of aggregates in representative areas of these histology sections (4°C). Statistical data revealed that heterozygous and homozygous lenses reduced numbers of aggregates by approximately 50% and 95%, respectively, compared with wild-type lenses (Fig. 4B). Consistent with the results of cold-induced protein aggregates, fresh homozygous lenses did not form cold cataracts, whereas fresh wild-type lenses displayed large and dense cold cataracts in PBS buffer at 4°C, but not at 37°C (Fig. 4C). Temperature-insensitive nuclear cataracts observed in homozygous mutant lenses probably resulted from abnormal light scattering caused by intranuclear aggregates and incomplete denucleation of inner fiber cells.

We further investigated whether the reduction in cold cataract formation was associated with the solubility of lens proteins. The amount of total, water-soluble, and water-insoluble proteins was measured in the lenses of wild-type and homozygous mutant mice at P5. There was a significant (approximately 30%) loss of water-soluble proteins in homozygous mutant lenses compared with wild-type lenses (Fig. 4D). The loss of soluble proteins in the homozygous lenses was accompanied by an increase of water-insoluble proteins. Thus, the reduction

of cold cataract formation was correlated to a loss of water-soluble proteins in the mutant lenses.

Sustained nuclei, nuclear remnants, and lens proteins aggregates cannot directly cause posterior rupture in homozygous γD (V76D/V76D) lenses. We hypothesize that lens rupture is a consequence of other downstream events resulting from aberrant nuclei or γ-crystallin aggregates. Our previous studies have shown that alterations of connexin proteins, the subunits of gap junction channels, lead to a variety of lens phenotypes, including nuclear cataracts, lens posterior rupture, and small lenses.[25] Therefore, we examined the levels of α3 (connexin 46) and α8 (connexin 50) connexins in mutant lenses. Western blotting confirmed reductions of α3 and α8 connexins, but not MP26 (aquaporin 0) or actin, in mutant lenses (Fig. 5A). Immunohistochemical staining further confirmed that connexins were mainly reduced in mature fiber cells at different ages. A representative staining result for α8 connexins detected by a polyclonal antibody is shown in Figure 5B.

Reduced Solubility of Mutant γD-V76D Proteins

To understand how this mutation leads to unique morphologic changes and the reduction of lens water-soluble proteins, we
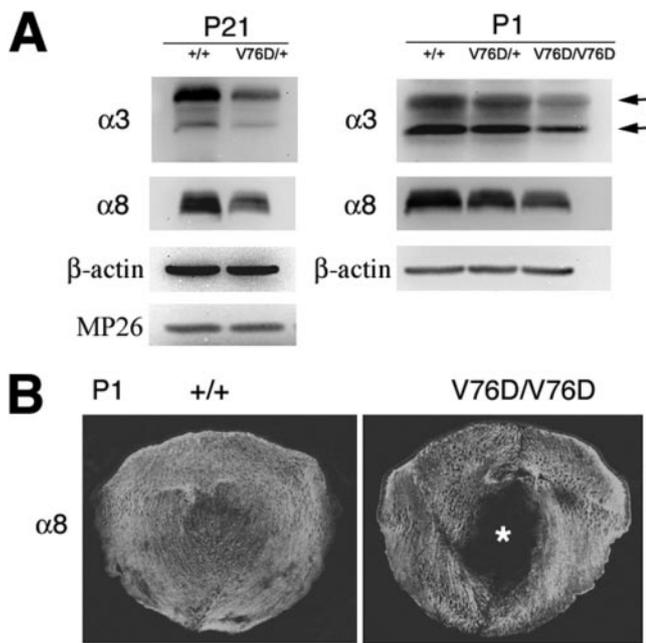
FIGURE 5. Mutant lenses have decreased levels of connexin protein. (**A**) Western blot results of lens water-insoluble proteins from P21 γD (+/+) and γD (V76D/+) mice and of P1 γD (+/+), γD (V76D/+) and γD (V76D/V76D) mice detected by antibodies against α3 connexin, α8 connexin, β-actin, or MP26 (aquaporin 0). *Top*: Upper bands are the phosphorylated form of α3 connexin, and lower bands are the unphosphorylated form (*arrows*). (**B**) Representative α8 connexin–immunostained lens sections from P1 γD (+/+) and γD (V76D/V76D) littermates. Fluorescent signals of α8 connexins were decreased in γD (V76D/V76D) lenses, especially in the inner fiber cells (*asterisk*). Scale bar, 200 μm.

examined the biochemical properties of crystallin proteins in mutant lenses. Gel filtration results of lens water-soluble proteins showed a significant reduction of the γ-crystallin peak in mutant lenses (Fig. 6A). Quantitative analysis of peak areas revealed an approximately 12% reduction of total water-soluble γ-crystallins in γD (V76D/+) lenses and an approximately 50% reduction in γD (V76D/V76D) lenses compared with that of wild-type γD (+/+) lenses.

Water-soluble and water-insoluble proteins of γD (+/+), γD (V76D/+), and γD (V76D/V76D) lenses of 1-week-old littermates were examined by two-dimensional electrophoresis (2-DE). The 2-DE data of water-soluble proteins were similar among different lens samples, except that the substituted aspartic acid residue caused the γD-V76D mutant protein spot to shift toward the acidic region (Fig. 6B, arrowheads) compared with the wild-type γD-crystallin protein spot. The calculated isoelectric point (pI) based on the full-length amino acid sequence of the protein is 6.72 for wild-type γD and 6.41 for mutant γD-V76D. Moreover, the amount of γD-V76D mutant proteins was lower than the amount of wild-type γD-crystallin proteins in lens water-soluble homogenates when comparing mutant and wild-type proteins from different alleles in heterozygous lenses (Fig. 6B, left middle) or when comparing homozygous (Fig. 6B, left bottom) and wild-type (Fig. 6B, left top) lens samples. Therefore, the data suggested that γD-V76D mutant proteins were less water soluble than wild-type γD-crystallin proteins in the lens.

The 2-DE data verified that the increased water-insoluble proteins in mutant lenses contained γD-V76D mutant protein and other crystallin proteins. γ-Crystallins were normally absent in the water-insoluble protein fraction of wild-type lenses

(Fig. 6B, right upper), whereas γD-V76D mutant proteins were obviously present in the water-insoluble fraction of γD (V76D/+) lenses (Fig. 6B, right middle). A higher level of γD-V76D mutant proteins was detected in the water-insoluble fraction of γD (V76D/V76D) lenses (Fig. 6B, right bottom). In addition, α- and β-crystallins and small amounts of other γ-crystallins were detected in the water-insoluble fractions of γD (V76D/V76D) lenses. Western blotting results also confirmed increased γ-crystallin proteins without cleaved γ-crystallin products in the water-insoluble fraction of mutant lenses (data not shown). These data further support that mutant γD-V76D proteins are less soluble in the lens.

Mutant Protein Aggregates in the Nucleus and the Cytosol of Transfected Cells

We tried to mimic the unique properties of γD-V76D mutant proteins in vitro and to further investigate how γD-V76D mutant proteins form intranuclear aggregates. Expression plasmids for wild-type γD or mutant γD-V76D proteins tagged with RFP at their C-terminal ends were transiently transfected into immortalized mouse lens epithelial cells. Wild-type γD-RFP proteins were detected in the nuclei and the cytosol without aggregation (Fig. 7A, top), and mutant γD-V76D-RFP proteins formed in nuclear and perinuclear aggregates of all transfected cells. These intranuclear aggregates disrupted the nuclei but did not colocalize with chromosomal DNA (Fig. 7A, middle and bottom). These results demonstrate that wild-type γD-crystallin proteins are present in the nuclei or the cytosol, whereas mutant γD-V76D proteins uniquely form nuclear aggregates to indirectly affect chromosomal DNA in the nucleus. Thus, these data recapitulated some of the properties of mutant γD-V76D proteins in vivo.

To confirm that the intranuclear aggregation of γD-V76D mutant proteins was a unique change rather than a general consequence of the expression of any mutant γ-crystallin protein in transfected cells, we also examined the γB-I4F mutant protein. It has been reported that γB-I4F mutation causes nuclear cataracts and that mutant γB-I4F proteins are less soluble and stable than the wild-type γB-crystallin proteins.[19] As were RFP-tagged wild-type γD-crystallin, RFP-tagged wild-type γB-crystallin proteins were detected in the nuclei and cytosol without aggregation in transfected cells (Fig. 7B, top). However, γB-I4F-RFP mutant proteins, observed in cytosol and nuclei, formed only cytosolic or perinuclear aggregates in approximately 30% of transfected cells (Fig. 7B, middle). No intranuclear aggregates of γB-I4F-RFP mutant proteins were observed, even when these mutant proteins were enriched in the nuclei of transfected cells (Fig. 7A, bottom). These results suggest a mechanistic difference for cataractogenesis between γD-V76D and γB-I4F mutations.

Structural Modeling of Mutant γD-V76D Proteins

To understand how the substituted aspartic acid residue causes γD-crystallin proteins to form aggregates and to become less water soluble, we performed structural modeling by using the Swiss model software to compare the structural information between wild-type and mutant proteins. The γD-V76D mutation is located in the random coiled structure of the first domain of the protein. Predicted tertiary structures show no significant difference between wild-type and mutant proteins. However, the substituted Asp76 forms two potential hydrogen bonds with Arg77 and Ser78 and alters the electrostatic potential of mutant proteins (Fig. 8).

DISCUSSION

This study reveals that γD-V76D mutant proteins are less soluble in the lens and form substantial intranuclear aggregates that
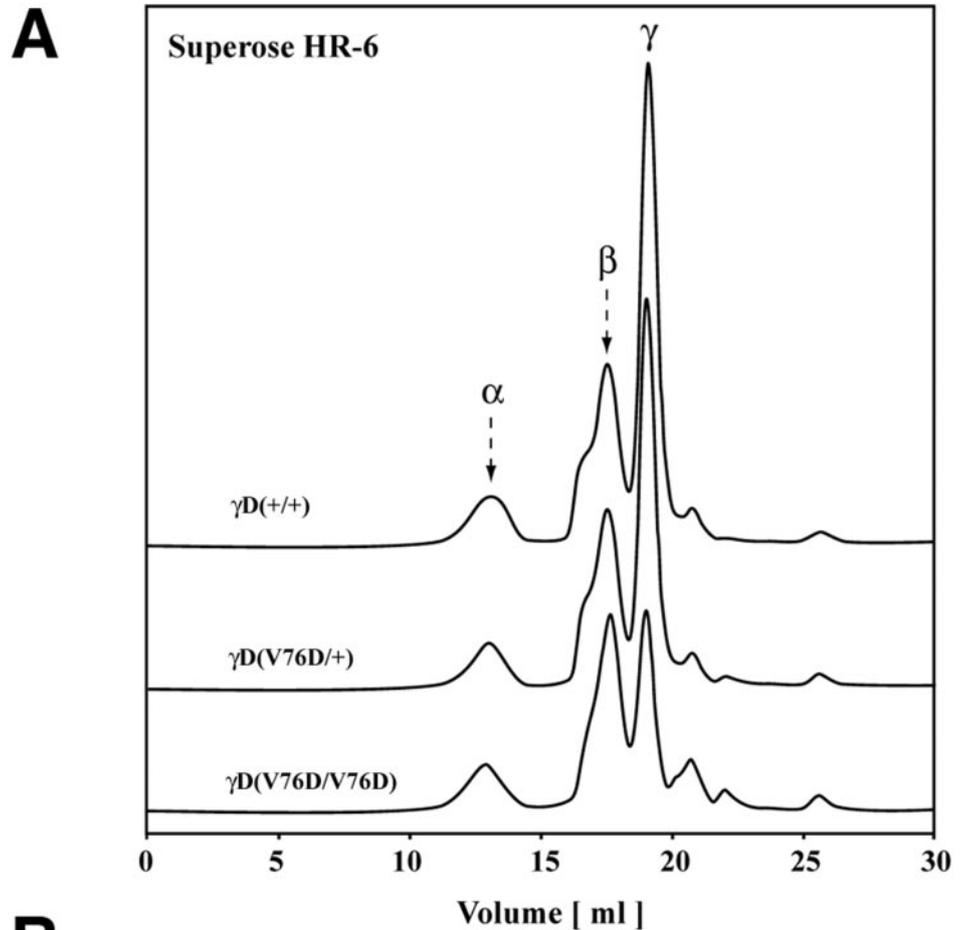
FIGURE 6. Mutant γD-V76D proteins predominantly become water insoluble in the lens. (**A**) Gel-filtration graphs of total lens water-soluble proteins of P7 wild-type γD (+/+), heterozygous γD (V76D/+), and homozygous γD (V76D/V76D) littermates. Peaks of α-, β-, and γ-crystallins are indicated. Quantitative analysis of these peak areas indicated that there was no difference in α-crystallin and β-crystallin peaks among different lenses. However, compared with wild-type lenses, analysis of the γ-crystallin peaks revealed an approximately 12% reduction in heterozygous lenses and an approximately 50% reduction in homozygous lenses. (**B**) Two-dimensional electrophoresis of water-soluble and water-insoluble lens proteins from P7 γD (+/+), γD (V76D/+), and γD (V76D/V76D) littermates. Protein spots for wild-type αA- and αB-crystallins are marked in all panels. Wild-type γ-crystallin isoforms (γA-γF) are labeled in the 2-DE panel of γD (V76D/+) water-soluble lens proteins (*middle left*). *Arrowheads* indicate spots of γD-V76D mutant protein. *Arrow* in the 2-DE panel of water-soluble γD (V76D/V76D) lens proteins (*bottom left*) indicates the absence of wild-type γD-crystallin proteins.
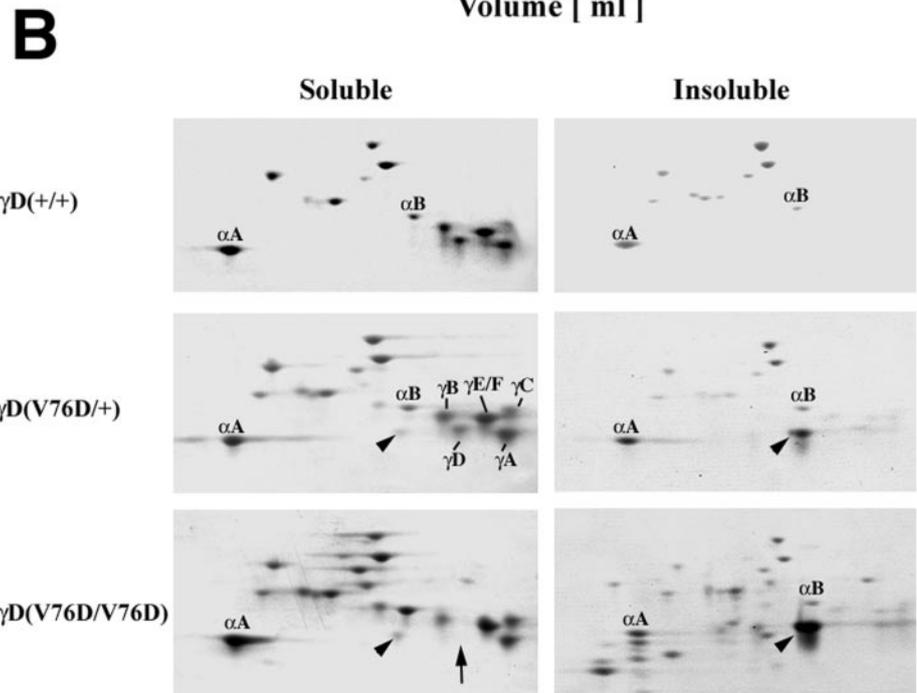
disrupt the denucleation process of inner lens fiber cells. Sustained cell nuclei or nuclear remnants can directly scatter light and probably cause other downstream changes, such as decreased connexin proteins that presumably inhibit gap junction communication to disrupt lens homeostasis. These molecular and cellular alterations directly or indirectly lead to the development of distinct cataracts in heterozygous and homozygous γD-V76D mice. This work provides new evidence that γD-crystallin proteins contribute to the formation of distinct cataracts and that the reduction of cold cataracts is correlated to a loss of lens water-soluble proteins. Therefore, γD-crystallin proteins, besides being structural components in the lens, may
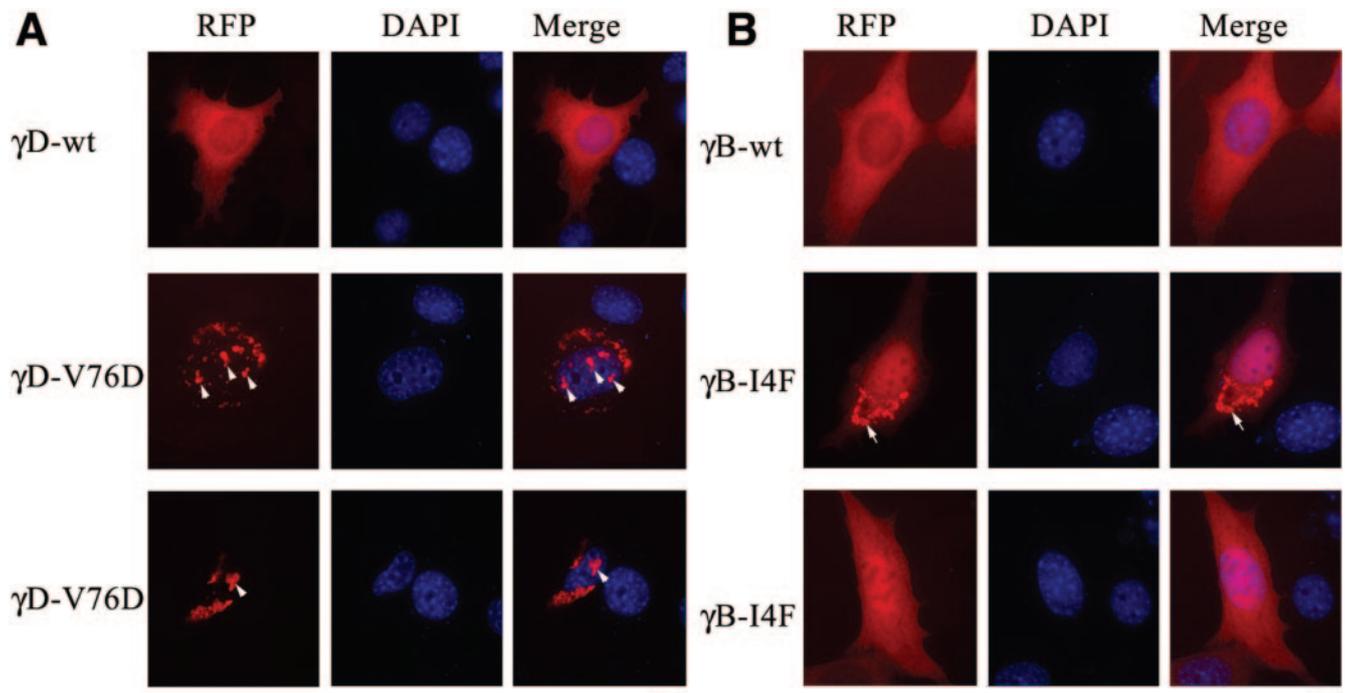
FIGURE 7. γD-V76D-RFP proteins form aggregates in the nucleus and the cytosol of transfected cells. (**A**) Plasmids expressing RFP-tagged wild-type γD-crystallin and mutant γD-V76D were transfected into immortalized mouse lens epithelial cells. Wild-type γD-RFP (γD-wt) proteins were detected in the nuclei and the cytosol without aggregation (*top*). Nuclei were stained by DAPI, but mutant γD-RFP (γD-V76D) proteins formed aggregates in the nuclei (*red spots* indicated by *white arrowheads*) and cytosol of all transfected cells. (**B**) Expression plasmids for RFP-tagged wild-type γB-crystallin and mutant γB-I4F were transfected into immortalized mouse lens epithelial cells. Wild-type γB-RFP (γB-wt) proteins were detected in the nuclei and cytosol without aggregation (*top*). However, mutant γB-RFP (γB-I4F) proteins formed cytosolic aggregates in approximately 30% of transfected cells (*red spots* indicated by *white arrow*, *middle left* and *right*). γB-I4F mutant proteins were abundant in the nuclei of all transfected cells without nuclear aggregates (*bottom*). Scale bars, 20 μm.

play important roles in the cytosol and in the nucleus to ensure proper maturation of lens fiber cells.

At least five different human γD mutations have been reported to cause different types of cataracts. The γD-R14C mutation causes dominant punctate cataracts[26]; in vitro biochemical studies suggest that cataracts are triggered by the thiol-mediated aggregation of R14C mutant proteins.[27] The γD-R58H mutation causes aculeiform cataracts,[28] and decreased solubility of mutant proteins probably trigger cataract formation.[29,30] The γD-R36S mutation facilitates the crystallization of mutant proteins, causing a cataract associated with macroscopically prismatic crystals.[31] Heterozygosity for a nonsense mutation, resulting in a truncated γD protein stopped at 156 (W156X), leads to nuclear cataracts.[32] The γD-P23T mutation leads to different types of cataracts, including lamellar cataracts, cerulean cataracts, coralliform cataracts, and fasciculiform and silicanlike nuclear cataracts in humans.[32-36] Studies of γD-P23T mutant proteins in vitro suggest a reduction of protein solubility, without any significant change of structure or stability.[37,38] Thus, different mutations of γD-crystallin can trigger distinct mechanisms to cause cataracts.

Although mutant proteins form intranuclear aggregates to cause cataracts, the γD-V76D mutation abolishes the formation of normal cytosolic aggregates (or cold cataracts) induced by low temperature. It has been reported that cytosolic aggregates of cold cataracts are composed of α-, β-, and γ-crystallins.[24] Our study suggested that a reduction of cold cataracts was correlated with decreased water-soluble proteins, including α-, β-, and γ-crystallins. Thus, one possible explanation is that mutant proteins perturb the interactions between α-, β-, and γ-crystallins to abolish the formation of cold cataracts. In vitro studies have demonstrated that γ-crystallins display temperature-dependent liquid-liquid phase separation.[39,40] Our present

study suggests that γD-crystallin is one of the essential components for the formation of cold cataracts. Structural modeling indicates that the substituted aspartic acid (D) residue of mutant γD-V76D alters hydrogen bonds and the electrostatic potential of mouse γD-crystallin protein, probably affecting its protein–protein interaction. It will be interesting to examine whether γD-V76D mutant proteins also lower the liquid–liquid phase separation temperature.

The γD-V76D mutation creates an intriguing situation when compared with other mutations. We have reported that γB-I4F mutant proteins had reduced stability and solubility.[19] However, γB-I4F mutant proteins only form cytosolic aggregates in vivo and in vitro, whereas mutant γD-V76D proteins form intranuclear aggregates. Truncated forms of γB-crystallin (*Crygb[nop]*, *Cat2[nop]*) or γE-crystallin (*Cryge[t]*, *Cryge[elo]*) have been reported to cause cataracts by forming intranuclear aggregates in lens primary fiber cells[41]; nuclear aggregation is suggested to result from a low level of α-crystallins in the nucleus.[41] However, our previous data reveal that mutant γB-I4F proteins bind to α-crystallins to form cytosolic aggregates in vivo and in vitro.[19] Therefore, α-crystallin cannot prevent the cytosolic aggregates of γB-I4F mutant proteins. Our current work also reveals that α-crystallin cannot prevent γD-V76D nuclear aggregates in lens secondary fiber cells in vivo. The 2-DE data of homozygous lenses show a substantial increase of water-insoluble γD-V76D mutant proteins without an increase of α-crystallins. Overexpression of αA-crystallin by cotransfection does not prevent cytosolic or nuclear aggregates of γD-V76D in transfected cells (data not shown). Therefore, this work suggests that α-crystallin selectively affects the aggregations of certain γ-crystallin mutants in the lens.

It is remarkable to identify an identical missense mutation reported previously from another screen of ENU-induced eye
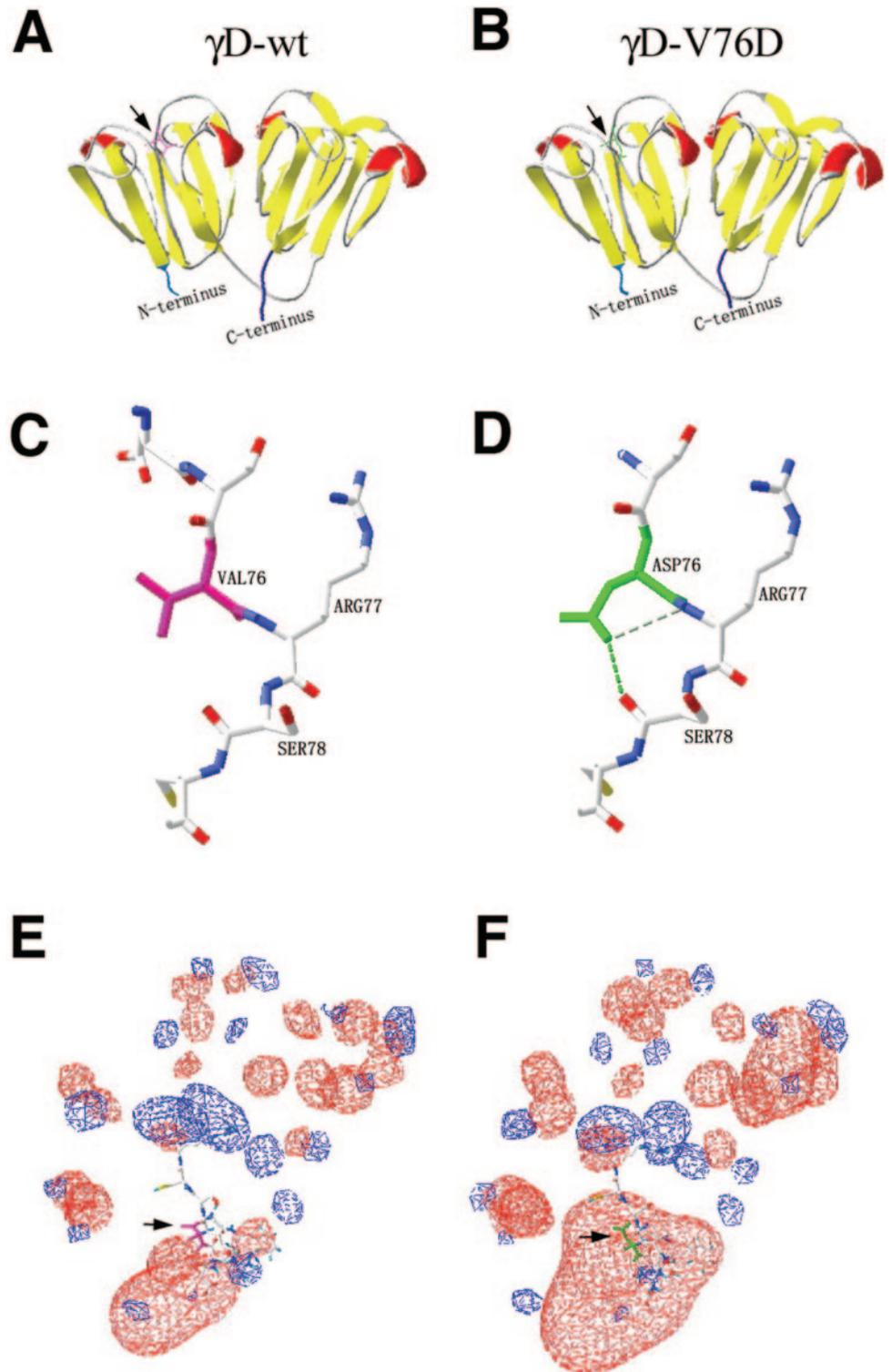
FIGURE 8. Structural modeling of the γD-V76D mutant protein using the Swiss model software. (**A**, **B**) Tertiary structures showed no significant difference between wild-type γD-crystallin and γD-V76D mutant proteins. *Arrows* indicate Val76 (*purple*) or Asp76 (*green*). (**C**, **D**) Unlike Val76 (*purple*) of the wild-type γD-crystallin, the substituted Asp76 (*green*) is predicted to form two hydrogen bonds (*dashed lines*) with Arg77 and Ser78 of the γD-V76D mutant protein. (**E**, **F**) Wild-type γD and mutant γD-V76D proteins had different predicted electrostatic potential maps. Negatively charged areas (*red*). Positively charged areas (*blue*). *Arrows* indicate Val76 (*purple*) or Asp76 (*green*).

mutations in the C3H strain background.[42] Thus, this is a hot spot for ENU-induced mutagenesis in the mouse genome. Interestingly, homozygous γD (V76D/V76D) mutant lenses in C3H strain background have incomplete denucleation without posterior rupture, similar to our heterozygous γD (V76D/+) mutant lenses in the B6 background. This phenotypic variation suggests the influence of genetic differences between the B6 and C3H strains. It is important to identify genetic modifiers that influence cataracts caused by γD-V76D mutation. Mouse

strain backgrounds also affect cataract severity in connexin mutant mice.[25,43,44] Our current data suggest that mutant γD-V76D crystallins indirectly decrease connexin protein levels in mutant lenses. Thus, the downstream events caused by γD-V76D mutant proteins or other factors that regulate cataractogenesis may be responsible for the phenotypic variation. γ-Crystallins are synthesized during the differentiation and maturation of lens fiber cells.[45,46] It is possible that γ-crystallin proteins play active roles in lens fiber cell maturation.

Acknowledgments

References

1. Bloemendal H, De Jong W, Jaenicke R, Lubsen NH, Slingsby C, Tardieu A. Ageing and vision: structure, stability and function of lens crystallins. *Prog Biophys Mol Biol*. 2004;86:407–485.

2. Piatigorsky J. Lens differentiation in vertebrates: a review of cellular and molecular features. *Differentiation*. 1981;19:134–153.

3. Bassnett S, Mataic D. Chromatin degradation in differentiating fiber cells of the eye lens. *J Cell Biol*. 1997;137:37–49.

4. Goodenough DA. The crystalline lens: a system networked by gap junctional intercellular communication. *Semin Cell Biol*. 1992;3: 49–58.

5. Mathias RT, Rae JL, Baldo GJ. Physiological properties of the normal lens. *Physiol Rev*. 1997;77:21–50.

6. Graw J, Loster J. Developmental genetics in ophthalmology. *Ophthalmic Genet*. 2003;24:1–33.

7. Nishimoto S, Kawane K, Watanabe-Fukunaga R, et al. Nuclear cataract caused by a lack of DNA degradation in the mouse eye lens. *Nature*. 2003;424:1071–1074.

8. Rong P, Wang X, Niesman I, et al. Disruption of Gja8 (alpha8 connexin) in mice leads to microphthalmia associated with retardation of lens growth and lens fiber maturation. *Development*. 2002;129:167–174.

9. Graw J, Neuhauser-Klaus A, Klopp N, Selby PB, Loster J, Favor J. Genetic and allelic heterogeneity of Cryg mutations in eight distinct forms of dominant cataract in the mouse. *Invest Ophthalmol Vis Sci*. 2004;45:1202–1213.

10. Foley JD, Rosenbaum H, Griep AE. Temporal regulation of VEID-7-amino-4-trifluoromethylcoumarin cleavage activity and caspase-6 correlates with organelle loss during lens development. *J Biol Chem*. 2004;279:32142–32150.

11. Weber GF, Menko AS. The canonical intrinsic mitochondrial death pathway has a non-apoptotic role in signaling lens cell differentiation. *J Biol Chem*. 2005;280:22135–22145.

12. Zandy AJ, Lakhani S, Zheng T, Flavell RA, Bassnett S. Role of the executioner caspases during lens development. *J Biol Chem*. 2005; 280:30263–30272.

13. Bassnett S. Lens fiber differentiation. In: Robinson ML, ed. *Development of the Ocular Lens*. Cambridge, UK: Cambridge University Press; 2004;214–244.

14. Horwitz J. Alpha-crystallin can function as a molecular chaperone. *Proc Natl Acad Sci USA*. 1992;89:10449–10453.

15. Derham BK, Harding JJ. Alpha-crystallin as a molecular chaperone. *Prog Retinal Eye Res*. 1999;18:463–509.

16. Slingsby C, Clout NJ. Structure of the crystallins. *Eye*. 1999;13(pt 3b):395–402.

17. Wistow G, Wyatt K, David L, et al. γN-crystallin and the evolution of the βγ-crystallin superfamily in vertebrates. *FEBS J*. 2005;272: 2276–2291.

18. Du X, Tabeta K, Hoebe K, et al. Velvet, a dominant Egfr mutation that causes wavy hair and defective eyelid development in mice. *Genetics*. 2004;166:331–340.

19. Liu H, Du X, Wang M, et al. Crystallin γB-I4F mutant protein binds to α-crystallin and affects lens transparency. *J Biol Chem*. 2005; 280:25071–25078.

20. Gong X, Li E, Klier G, et al. Disruption of α3 connexin gene leads to proteolysis and cataractogenesis in mice. *Cell*. 1997;91:833–843.

21. Sun P, Dong P, Dai K, Hannon GJ, Beach D. p53-Independent role of MDM2 in TGF-β1 resistance. *Science*. 1998;282:2270–2272.

22. Halbert CL, Demers GW, Galloway DA. The *E6* and *E7* genes of human papillomavirus type 6 have weak immortalizing activity in human epithelial cells. *J Virol*. 1992;66:2125–2134.

23. Joneson T, White MA, Wigler MH, Bar-Sagi D. Stimulation of membrane ruffling and MAP kinase activation by distinct effectors of RAS. *Science*. 1996;271:810–812.

24. Lo WK. Visualization of crystallin droplets associated with cold cataract formation in young intact rat lens. *Proc Natl Acad Sci USA*. 1989;86:9926–9930.

25. Chang B, Wang X, Hawes NL, et al. A Gja8 (Cx50) point mutation causes an alteration of α3 connexin (Cx46) in semi-dominant cataracts of Lop10 mice. *Hum Mol Genet*. 2002;11:507–513.

26. Stephan DA, Gillanders E, Vanderveen D, et al. Progressive juvenile-onset punctate cataracts caused by mutation of the γD-crystallin gene. *Proc Natl Acad Sci USA*. 1999;96:1008–1012.

27. Pande A, Pande J, Asherie N, et al. Molecular basis of a progressive juvenile-onset hereditary cataract. *Proc Natl Acad Sci USA*. 2000; 97:1993–1998.

28. Heon E, Priston M, Schorderet DF, et al. The gamma-crystallins and human cataracts: a puzzle made clearer. *Am J Hum Genet*. 1999; 65:1261–1267.

29. Pande A, Pande J, Asherie N, et al. Crystal cataracts: human genetic cataract caused by protein crystallization. *Proc Natl Acad Sci USA*. 2001;98:6116–6120.

30. Basak A, Bateman O, Slingsby C, et al. High-resolution X-ray crystal structures of human γD crystallin (1.25 A) and the R58H mutant (1.15 A) associated with aculeiform cataract. *J Mol Biol*. 2003;328: 1137–1147.

31. Kmoch S, Brynda J, Asfaw B, et al. Link between a novel human γD-crystallin allele and a unique cataract phenotype explained by protein crystallography. *Hum Mol Genet*. 2000;9:1779–1786.

32. Santhiya ST, Shyam Manohar M, Rawlley D, et al. Novel mutations in the gamma-crystallin genes cause autosomal dominant congenital cataracts. *J Med Genet*. 2002;39:352–358.

33. Nandrot E, Slingsby C, Basak A, et al. γ-D crystallin gene (CRYGD) mutation causes autosomal dominant congenital cerulean cataracts. *J Med Genet*. 2003;40:262–267.

34. Xu WZ, Zheng S, Xu SJ, Huang W, Yao K, Zhang SZ. Autosomal dominant coralliform cataract related to a missense mutation of the γD-crystallin gene. *Chin Med J (Engl)*. 2004;117:727–732.

35. Mackay DS, Andley UP, Shiels A. A missense mutation in the γD crystallin gene (*CRYGD*) associated with autosomal dominant "coral-like" cataract linked to chromosome 2q. *Mol Vis*. 2004;10: 155–162.

36. Burdon KP, Wirth MG, Mackey DA, et al. Investigation of crystallin genes in familial cataract, and report of two disease associated mutations. *Br J Ophthalmol*. 2004;88:79–83.

37. Evans P, Wyatt K, Wistow GJ, Bateman OA, Wallace BA, Slingsby C. The P23T cataract mutation causes loss of solubility of folded γD-crystallin. *J Mol Biol*. 2004;343:435–444.

38. Pande A, Annunziata O, Asherie N, Ogun O, Benedek GB, Pande J. Decrease in protein solubility and cataract formation caused by the Pro23 to Thr mutation in human γD-crystallin. *Biochemistry*. 2005;44:2491–2500.

39. Siezen RJ, Fisch MR, Slingsby C, Benedek GB. Opacification of gamma-crystallin solutions from calf lens in relation to cold cataract formation. *Proc Natl Acad Sci USA*. 1985;82:1701–1705.

40. Clark JI, Clark JM. Lens cytoplasmic phase separation. *Int Rev Cytol*. 2000;192:171–187.

41. Sandilands A, Hutcheson AM, Long HA, et al. Altered aggregation properties of mutant gamma-crystallins cause inherited cataract. *EMBO J*. 2002;21:6005–6014.

42. Graw J, Loster J, Soewarto D, et al. V76D mutation in a conserved gD-crystallin region leads to dominant cataracts in mice. *Mamm Genome*. 2002;13:452–455.

43. Runge PE, Hawes NL, Heckenlively JR, Langley SH, Roderick TH. Autosomal dominant mouse cataract (Lop-10): consistent differences of expression in heterozygotes. *Invest Ophthalmol Vis Sci*. 1992;33:3202–3208.

44. Gong X, Agopian K, Kumar NM, Gilula NB. Genetic factors influence cataract formation in alpha 3 connexin knockout mice. *Dev Genet*. 1999;24:27–32.

45. Treton JA, Jacquemin E, Courtois Y, Jeanny JC. Differential localization by in situ hybridization of specific crystallin transcripts during mouse lens development. *Differentiation*. 1991;47:143–147.

46. Ueda Y, Duncan MK, David LL. Lens proteomics: the accumulation of crystallin modifications in the mouse lens with age. *Invest Ophthalmol Vis Sci*. 2002;43:205–215.